Solid State Science and Technology, Vol. 20, No 1& 2 (2012) 1-10
ISSN 0128-7389

INFLUENCE OF SINTERING TEMPERATURE ON MICROSTRUCTURAL, ELECTRICAL AND MAGNETO-TRANSPORT OF $Nd_{0.68}Sr_{0.32}MnO_3$

L.S. Ewe[1,*], A.Jemat[1], W. N. Voon[1] and K.P.Lim[2]

[1]*College of Foundation and General Studies, Universiti Tenaga Nasional, Kampus Putrajaya, Jalan IKRAM-UNITEN, 43000 Kajang, Selangor, Malaysia*

[2]*Department of Physics, Faculty of Science, Universiti Putra Malaysia, 43300 UPM Serdang, Selangor, Malaysia*

**Corresponding author: laysheng@uniten.edu.my*

ABSTRACT

A systematic study on $Nd_{0.68}Sr_{0.32}MnO_3$ manganites has been undertaken, primarily to understand the influence of varying grain size on the structural, electrical resistivity and magneto transport properties at the insulating and metallic regions. The materials were prepared by the solid state reaction method at sintering temperature 1170 ^oC, 1270 ^oC and 1350 ^oC. The XRD patterns show all samples have a single phase with orthorhombic structure. SEM images show a linear relationship between sintering temperature and grain size. The insulator metal transition temperatures, T_{im} were determined and remained nearly constant (~ 200 K) for samples sintered at 1270 ^oC and 1350 ^oC. While for sample sintered at 1170 ^oC, T_{im} is found around 180 K. The resistivity data fits well with equations $\rho = \rho_o + \rho_2 T^2$ and $\rho = \rho_o + \rho_{2.5} T^{2.5}$ in metallic (ferromagnetic) region. At high temperature ($T>T_{im}$) insulating (paramagnetic) region, small polaron hopping and variable range hopping models were used to compute the density of states at Fermi level $N(E_F)$ and the activation energy (E_a) of the electrons.

Keywords: magnetotransport; grain size; activation energy

INTRODUCTION

Recently, there have been many studies of the manganese oxides, $R_{1-x}A_xMnO_3$ (R = La, Pr, Nd; A = Ca, Sr, Ba, Pb), where colossal magnetoresistance (CMR) effect has been reported [1]. The parent insulator $RMnO_3$ contains Mn^{3+} ions with a $t^3_{2g}\, e^1_g$ (total spin $S = 2$) electronic configuration. The substitution of R^{3+} with a divalent element A^{2+} results in a mixed valency of Mn^{3+} ($t^3_{2g}\, e^1_g : S = 2$) and Mn^{4+} ($t^3_{2g} : S = 3/2$) ions. Their interaction is responsible for the metallic and ferromagnetic properties of $R_{1-x}A_xMnO_3$ due to the double exchange (DE) mechanism [2]. Mn^{4+} lacks of e_g electron and hence the itinerant hole associated with the Mn^{4+} ions may hop to Mn^{3+}. However, due to a strong on-site exchange interaction (Hund's rule) with the localized Mn electrons, only hoping between sites with localized parallel spins is favored [3]. This is the essence of double exchange model and is used to explain the physical nature of the interaction and

the simultaneous occurrence of ferromagnetism and metalic nature of the material below insulator-metal transition temperature (T_{im}). The overlap of O p- and Mn d-orbitals depends on Mn-Mn distance and Mn-O-Mn angle that can be modified by varying the average size of ions at Mn site [4]. The concentration of Mn^{3+} and Mn^{4+} ions can be controlled by changing the A doping level or the oxygen stoichiometry [5]. The insulating $x = 0$ phase changes to a metallic and ferromagnetic phase for ~0 .2 < x < ~0.5 [6, 7].

Recent studies on these materials revealed that CMR phenomenon is attributed not only to the double exchange (DE) mechanisme but also to the interactions such as electron-phonon coupling, electron-magnon interaction, and the complicated band structure [3, 8]. By using sol-gel process, with increasing sintering temperatures in $Nd_{0.67}Sr_{0.33}MnO_3$ perovskites, the insulator-metal transition temperature (T_{im}) increases from 215 K to 245 K [9]. The grain size increased with the increasing temperature of sintering from ~0.1 μm at 1173 K to ~2.1 μm at 1673 K. It is well known that change in the grain size has direct consequence on the electronic and magneto-transport properties of a system [10]. Increase of sintering temperature induced the formation of an interfacial phase near the grain boundaries in $La_{0.67}Sr_{0.33}MnO_3$ and $Nd_{0.67}Sr_{0.33}MnO_3$ [11]. Therefore, the influence of varying grain size on structural, electrical resistivity and magneto transport properties of $Nd_{0.68}Sr_{0.32}MnO_3$ at different sintering temperatures are reported here.

EXPERIMENTAL DETAILS

The polycrystalline $Nd_{0.68}Sr_{0.32}MnO_3$ samples were prepared by standard solid state reaction state method with high-purity of Nd_2O_3, $SrCO_3$ and MnO. The samples were mixed, ground carefully and calcined at 850 ^oC and 900 ^oC in furnace for 12 hours and then cooled to room temperature at 2 ^oC/min. The powders were reground, pressed into circular pellets and sintered at 1170 ^oC, 1270 ^oC and 1350 ^oC.

The data was then collecting in a 2θ range of 20-70°. The phase purity and crystal structure of samples were verified by X-ray diffraction (XRD) using a Siemens D5000 diffractometer with CuK_α radiation (λ = 1.5418 Å) at room temperature. Scanning electron microscopy (SEM) was used to determine the surface morphology of the samples. Electrical resistivity in the temperature range of 30 - 300 K was measured by using the standard four-probe method with silver paste contacts in conjunction with a closed cycle refrigerator from CTI Cryogenics (model 22) and a temperature controller from Lake Shore (model 330).

RESULTS AND DISCUSSION

The XRD patterns of all samples (Figure 1) are found to be in single phase with orthorhombic structure (space group: *lmma*) without any impurity phases. No peak shifting in the XRD patterns was observed, while the relative intensities of the peak changes slightly. This indicates that the sintering temperature does not affect the lattice

parameter [11] but thus affect the Mn-O-Mn bond angle, which can dominate the electronic properties, such as T_{im}.

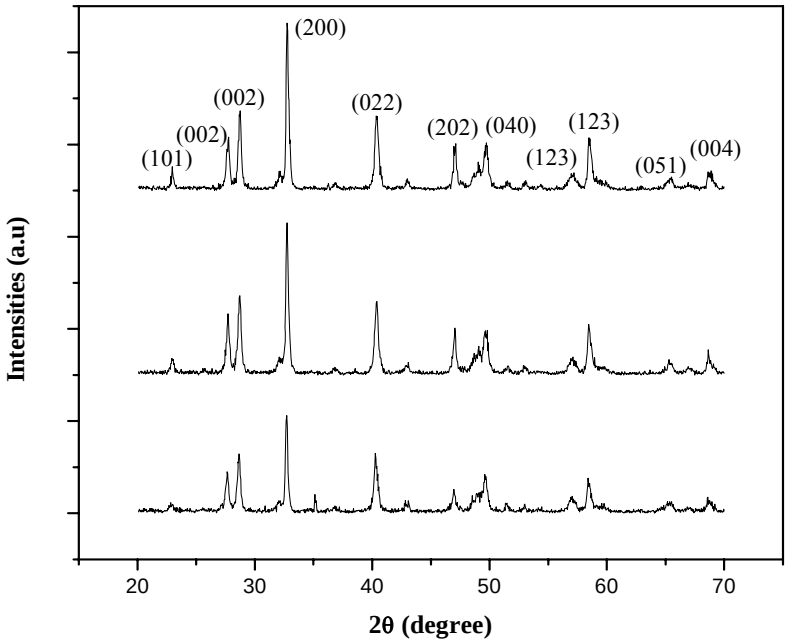

Figure 1: X-ray diffraction patterns of $Nd_{0.68}Sr_{0.32}MnO_3$ with different sintering temperature

It can be seen from SEM micrograph in Figure 2 that there is an obvious variation in grain size as the sintering temperature was increased from 0.96 μm at 1170 ^oC to 1.22 μm at 1270 ^oC, and 1.40 μm at 1350 ^oC. It can be seen a spiral grains grew pattern along a favorable orientation for sample sintered at 1270 ^oC (Figure 2 (b)). Sample sintered at 1350 ^oC has well-formed crystallites with the largest grain size as compared with samples sintered at 1170 ^oC and 1270 ^oC. The effect of grain size on charge-ordering and phase segregation of $Nd_{0.5}A_{0.5}MnO_3$ (A= Ca, Sr) showed that sample with smaller grain size that sintered at 1173 K has greater ferromagnetic (FM) interaction at lower temperature due to phase segregation, compared to the sample with the largest grain size that sintered at 1673 K [12].

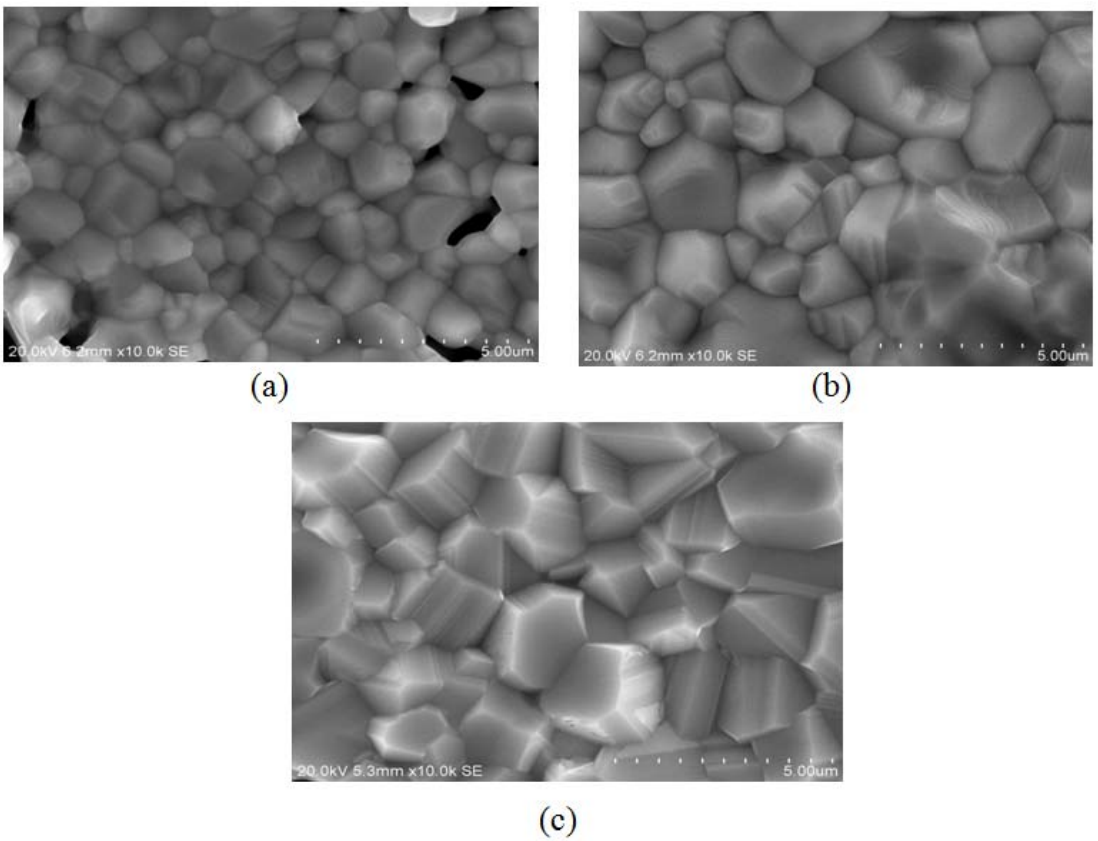

Figure 2: SEM micrographs of $Nd_{0.68}Sr_{0.32}MnO_3$ sintered at (a) 1170 ^oC, (b) 1270 ^oC, and (c) 1350 ^oC

Figure 3 shows the temperature dependence of resistivity for $Nd_{0.68}Sr_{0.32}MnO_3$ at 1170 °C, 1270 °C, and 1350 °C. Insulator metal transition temperature, T_{im} for sample sintered at 1170 ^oC was around 180 K. Whereas, T_{im} for samples sintered at 1270 ^oC and 1350 ^oC were almost constant (~ 200 K). From microscopic point of view, manganite systems contain metallic ferromagnetic domains linked with paramagnetic insulating regions. Decreasing of grain size relatively increases the insulating regions, making resistivity large and thereby lowering T_{im} [13]. The T_{im} for $Nd_{0.5}Sr_{0.5}MnO_3$ prepared by sol-gel method and sintered at 1100 ^oC was reported to be around 245 K [13]. T_{im} values were very dependent on the diffusion process that controls the growth of the grain [14]. The spiral growth of grain size caused the increasing of T_{im} for samples sintered at 1270 ^oC but does not enhance its resistivity. The decrease in grain size increased the magnetically disordered states on the surface of the grains therefore double exchange (DE) mechanism was weakened and resistivity was enhanced [15]. However, our results showed that sample sintered at 1350 ^oC gave the largest grain size and formed crystallite very well as T_{im} shifted to higher temperature, which were around 204 K. Grain boundary may play a dominant role in enhancing the scattering of the conducting electron in this sample. This may decreased the density of ferromagnetic metallic

(FMM) particles consequently lowered the T_{im} and enhanced the electrical resistivity. The shift of T_{im} towards higher temperature region can be explained as the enhancement of grain growth that improved the connectivity between the grains.

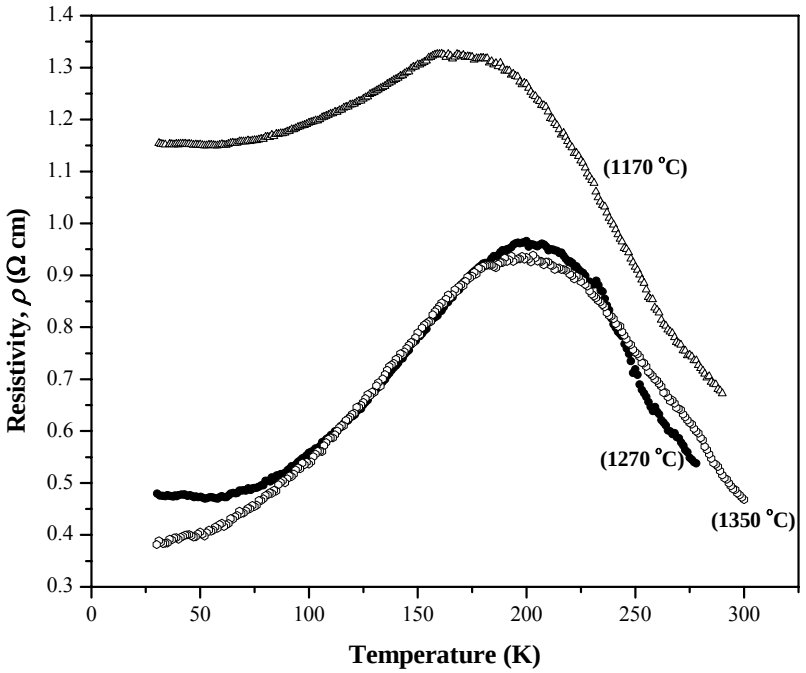

Figure 3: Resistivity versus temperature of $Nd_{0.68}Sr_{0.32}MnO_3$ at 1170 ^oC, 1270 ^oC, and 1350 ^oC.

In order to explain the transport mechanisms in the whole range of the measuring temperature, we fitted the ρ-T curves according to several equations and models. The electrical resistivity data at low temperatures ($T<T_{im}$) can be fitted to $\rho = \rho_o + \rho_2 T^2$ and $\rho = \rho_o + \rho_{2.5} T^{2.5}$ where the term ρ_o represents resistivity due to the grain boundary effects, the term $\rho_2 T^2$ is due to the electron-electron scattering process [3, 8] and $\rho_{2.5} T^{2.5}$ represents resistivity due to single magnon scattering process in ferromagnetic phase [3, 15]. Figure 4(a) and 4(b) shows the resistivity data fitted to $\rho = \rho_o + \rho_2 T^2$ and $\rho = \rho_o + \rho_{2.5} T^{2.5}$ while ρ_2 and $\rho_{2.5}$ values are tabulated in Table 1. As we can see, ρ_o, ρ_2 and $\rho_{2.5}$ values decrease with an increase in grain size. The enlargement of grain size may decrease the grain boundary region and hence, the net grain boundary [8]. The grain boundary region decreased as a result of an increase in the grain size which can explain why the net grain boundary plays the dominant role in the conduction process [3, 9]. ρ-T^2 and ρ-$T^{2.5}$ curves show the resistivity data is fitted very well due to high linear correlation coefficient value (R^2) in the ρ-T^2 and ρ-$T^{2.5}$ curves (Table 1).

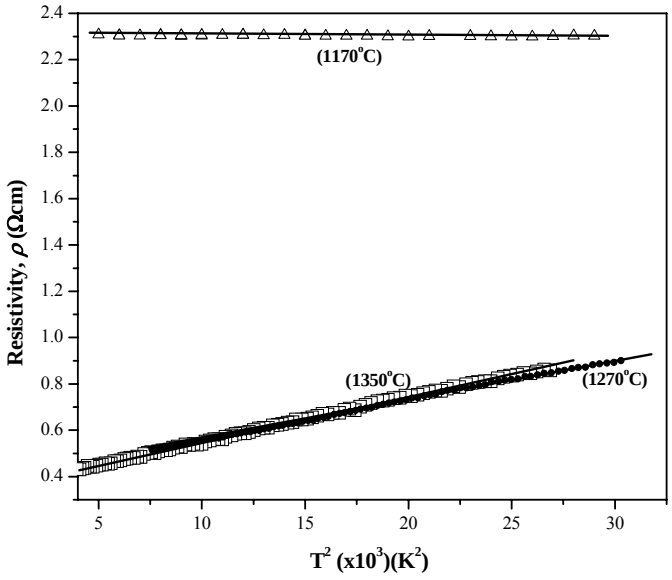

(a)

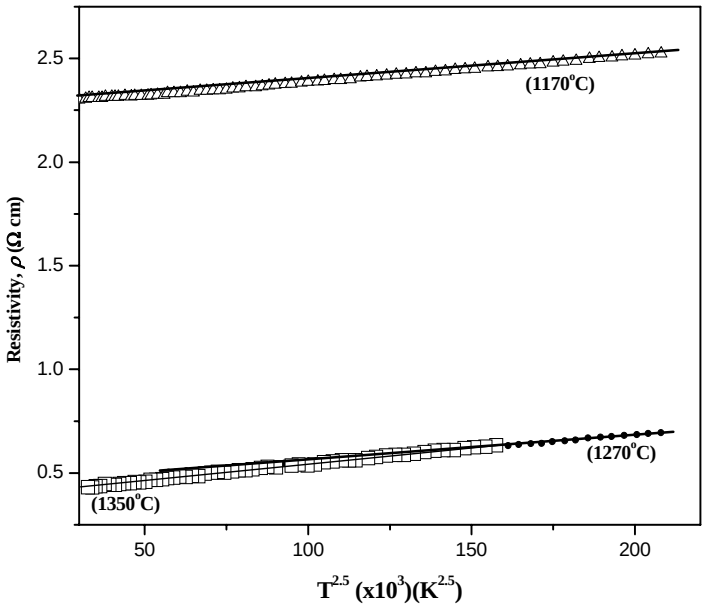

(b)

Figure 4: Resistivity vs. temperature below T_{im} of $Nd_{0.68}Sr_{0.32}MnO_3$ with solid line fitted with (a) $\rho = \rho_0 + \rho_2 T^2$ and (b) $\rho = \rho_0 + \rho_{2.5} T^{2.5}$ at sintering temperature 1170 ^oC, 1270 ^oC, and 1350 ^oC

Table 1: $\rho_{2,}$ $\rho_{o,}$ R^2_2 (linear correlation coefficient), $\rho_{2.5,}$ ρ_o and $R^2_{2.5}$ of $Nd_{0.68}Sr_{0.32}MnO_3$ sintered at 1170 ^oC, 1270 ^oC, and 1350 ^oC

Sintering Temperature (°C)	ρ_0 **Ωcm**	ρ_2 **ΩcmK^{-2}**	$\mathbf{R^2_2}$	ρ_0 **Ωcm**	$\rho_{2.5}$ **ΩcmK$^{-2.5}$**	$\mathbf{R^{2.5}_{2.5}}$
1170	1.839	19.1	0.9974	2.3020	1.6	0.9980
1270	0.379	17.6	0.9988	0.4290	1.3	0.9992
1350	0.356	3.0	0.9985	0.3810	1.1	0.9970

It is interesting to note that the values of R^2 are found to be equal or greater than 0.98 for all samples. The increments of ρ^2 and $\rho^{2.5}$ values indicate the increase of electron-spin fluctuations in the samples with the decrease in sintering temperature [8]. It means that both of these parameters decrease with increasing grain size, which may be the evidence for the decrease of scattering processes due to the enlargement of the material [13].

To understand the high temperature resistivity data (above T_{im}), variable range hopping model (T_{im}< T< Θ_D/2) and small polaron hopping (T > Θ_D/2) are generally used [13]. The activation energy (E_a) and the density of states at Fermi level ($N(E_F)$) can be calculated from the slope of the graph ln (ρ/T) versus T^{-1}(Figure 5(a)) and from the graph ln (ρ) versus $T^{-0.25}$(Figure 5(b)).

The values of activation energy (E_a) and density of state at Fermi level $N(E_F)$ are shown in Table 2. It can be seen from Table 2 that T_o values are found to decrease with increasing sintering temperature. The increase of sintering temperature led to the decrease in the T_o values, where higher T_o values indicate an increase in bending of Mn-O-Mn bond angle With an increase in grain size, the interconnectivity between grains increases, which enhances the possibility of conduction electron to hop to the neighboring sites, thereby was decreasing the value of E_a [3]. However, in our work here the samples sintered at 1270 °C showed the highest of E_a value. This may due to existence of pore and void. The value of $N(E_F)$ is found the highest for sample 1270 °C too and while the sample with the largest grain size showed the lowest $N(E_F)$ value. The $N(E_F)$ reflects the carrier effective mass (or narrowing of the band-with), which in turn results in a drastic change in the resistivity and sharpening of the resistivity peak at the vicinity of T_{im} [8].

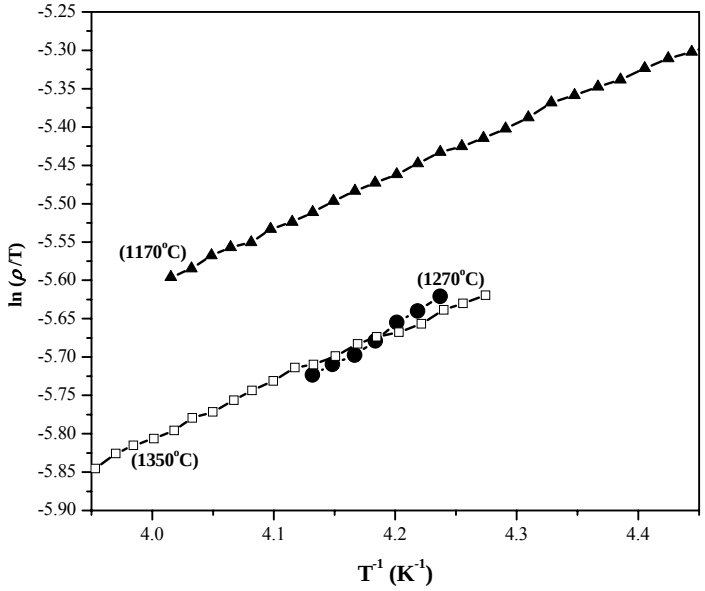

(a)

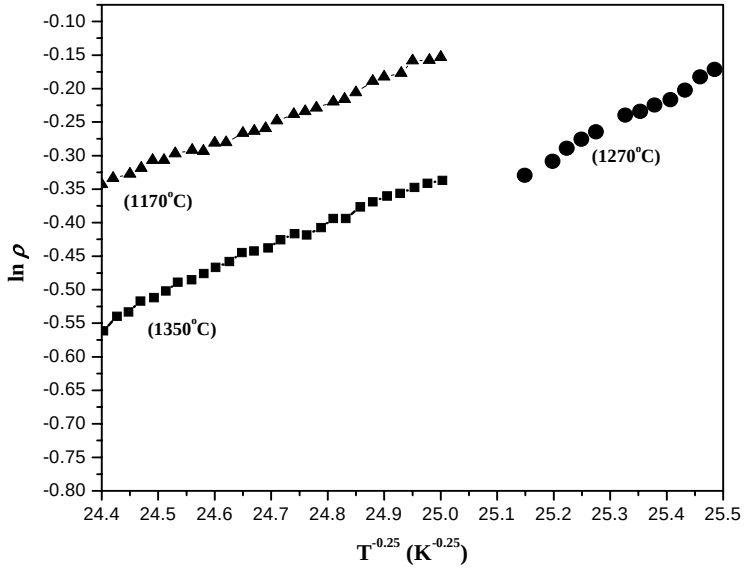

(b)

Figure 5: (a) ln(ρ/T) vs. T^{-1} of $Nd_{0.68}Sr_{0.32}MnO_3$ with solid line fitted with $\rho_{SPH} = \rho_o \exp(E_a/k_BT)$ and (b) ln(ρ) vs. $T^{-0.25}$ of $Nd_{0.68}Sr_{0.32}MnO_3$ with solid line fitted with $\rho_{VPH} = \rho_o \exp(T_o/T)$ at sintering temperature 1170 °C, 1270 °C, and 1350 °C

Table 2: Pre-factor (ρ_o), activation energy (E_a), T_o and density of states at the Fermi level ($N(E_F)$) of $Nd_{0.68}Sr_{0.32}MnO_3$ sintered at 1170 ^oC, 1270 ^oC, and 1350 ^oC

Sintering Temperature (°C)	ρ_o **(Ω cmK^{-1})**	E_a **(meV)**	T_o **(10^{-10}) (K)**	$N(E_F)$ **(eV^{-1}cm^{-3})**
0.12	1.21 x 10^{-3}	0.04	0.24	3.70 x 10^{-20}
0.152	5.49 x 10^{-5}	0.09	1.24	4.21 x 10^{-20}
0.22	1.84 x 10^{-4}	0.06	0.28	17.23 x 10^{-20}

CONCLUSION

As conclusion, the electrical resistivity at low temperature ($T<T_{im}$) regions can be attributed to electron-electron scattering and single magnon scattering process. At high temperature region ($T>T_{im}$), the resistivity may be explained by the adiabatic small polaron and variable range hopping mechanisms. Grain size was found to increase with increasing of sintering temperature. Therefore, it may conclude that the grain growth mechanism may affect the electrical, micstructural and magneto-transport properties but not on the structure of the materials. High sintering temperature helps to promote the grain growth of NSMO, grains become more compact and well crystallite form and hence shifted T_{im} to higher temperature range.

ACKNOWLEDGEMENT

The authors thank the Ministry of Higher Education of Malaysia under Fundamental Research grant no. FRGS/FASA 1-2009/SAINS TULEN/UNITEN/104 for supporting the research work.

REFERENCES

[1] R. yon Helmolt, J. Weckerg, B. Holzapfel, L. Schultz and K. Samwer, *Phys. Rev. Lett*. **71** (1993) 2331
[2] S. Jin, T.H. Tiefel, M. McCormack, R.A. Fastnacht, R. Ramesh and L.H. Chen, *Science* **264** (1994) 413
[3] G.Venkataiah, D.C.Krishna, M.Vithal, S.S.Rao, S.V.Bhat, V.Prasad, S.V.Subramanyam, P.Venugopal Reddy, *Physica B* **357** (2005) 370
[4] C.N.Rao and A.K. Raychaudhuri, (1998) *Colossal Magnetoresistance, Charge Ordering and Other Novel Properties of Manganates and Related Materials*, (World Scientific Singapore).
[5] H.L. Ju, J. Gopalakrishnan, J.L. Peng, Qi Li, G.C. Xiong, T. Venkatesan and R.L. Greene, *Phys. Rev. B* **51** (1995) 6143
[6] G.H. Jonker and J.H. van Santen, *Physica* **16** (1950) 337
[7] J. Volgar, *Physica* **20** (1954) 49

[8] L.S. Ewe, I. Hamadneh, H. Salama, N.A. Nasri, S.A. Halim, R. Abd-Shukor, *Appl Phys A* **95** (2009) 457-463
[9] R. Mahendiran, R. Mahesh, A.K. Raychaudhuri, C.N.R. Rao, *Solid State Commun*. **99** (3) (1996) 149
[10] A. Banerjee, S. Pal, S. Bhattacharya, B.K. Chaudhuri, *J. Appl. Phys*. **91** (2002) 5125
[11] Y.L. Change and C. K. Ong, *J. Phys Condens. Matter* **16** (2004) 3711
[12] L. Sudheendra, H.D. Chinh, A.R. Raju, A.K. Raychaudhuri, C.N.R. Rao, *Solid State Comm*. **122** (2002) 53
[13] G. Venkataiah, P. Venugopal Reddy, *J. Magn. Magn. Mater*. **285** (2005) 343-352
[14] P. Kameli, H. Salamati, A. Aezami, *J. Alloys Compd*. **450** (2008) 7
[15] B. Boy and S. Das, *J. Appl. Phys*. **104** (2008) 103915
[16] Y.B. Zhang, S. Li, C.Q. Sun, S. Widjaja, P. Hing, *Journal of MaterialsProcessing Technology* **122** (2002) 266-271